

Selective crystal growth of indium selenide compounds from saturated solutions grown in a selenium vapor

Chao Tang*^{1,2}, Yohei Sato¹, Katsuya Watanabe¹, Tadao Tanabe^{1,3}, Yutaka Oyama¹

¹ *Department of Materials Science, Graduate School of Engineering, Tohoku University*

² *Research institute of electrical communication, Tohoku University*

³ *Graduate School of Science and Engineering, Shibaura Institute of Technology*

Abstract: Indium selenide compounds are promising materials for energy conversion, spintronic applications, and chemical sensing. However, it is difficult to grow stoichiometric indium selenide crystals due to the high equilibrium selenium vapor pressure and the complicated phase equilibrium system of indium selenide compounds. In this paper, we apply a novel and convenient crystal growth method, in which the saturated solution is grown by the application of a selenium vapor. In this method, selenium vapor at a pressure higher than the saturated vapor pressure is applied to molten indium, such that the selenium continuously dissolves into the indium solution until the solubility at the growth temperature is reached; then a slow cooling process results in crystallization. The selenium dose is matched to its solubility so that indium selenide compounds can be selectively grown just by controlling the temperature without the need to consider the chemical ratio in the solution. The pressure of the vapor is controlled during the whole growth process so that any deviation from a stoichiometric composition in the crystal can be controlled. Both InSe and In₂Se₃ were successfully grown using this method, and we have investigated the

growth mechanism and found the growth window for each compound. This study presents a novel and convenient approach to fabricating transitional metal chalcogenides without deficiencies in the chalcogen element.

* Corresponding Author: tang.chao.c4@tohoku.ac.jp

Research Institute of Electrical Communication, Tohoku University. 2-1-1 Katahira, Aobaku, Sendai, 980-8577 Japan

1. Introduction

Transition-metal monochalcogenide (TMM) materials have been attracting increasing attention owing to their favorable properties [1-4]. Indium selenide compounds are typical TMMs, and have a narrow bandgap compared with transition metal sulfides and gallium compounds. The indium selenide compounds attracting most attention are InSe, In₂Se₃, and In₄Se₃. The bandgap energy of InSe and In₂Se₃ is about 1.3 eV, which makes them potential candidates for the next-generation of solar energy harvesting devices [5, 6] and highly-sensitive infrared detectors [7-9]. Also, InSe is considered to be a possible candidate for exploring the frontiers of spintronics [10, 11]. Moreover, InSe can be used for the adsorption of carbon oxide [12, 13]. Furthermore, In₄Se₃ has been reported as being a high-performance thermoelectric material with a considerable Seebeck coefficient of 1.48 [13].

Up to now, indium selenide crystals have been usually prepared by the Bridgman technique [6, 14-26]. The Bridgman technique has the following disadvantages, which limit the crystallinity of

the crystals. Firstly, crystals are grown from a molten mixture of In and Se where the temperature is much higher than the melting point of the growing crystal. Thermal motion of the molecules is induced by defects in the crystal [27]. Also, the vapor pressure of selenium during growth is high so that saturated selenium evaporates from the melt during growth, causing the composition of the crystal to be non-stoichiometric [28, 29]. Hence, the ratio of the elements in the melts used in the Bridgman method always differ from the stoichiometry of the target compound itself [30]. As a result, Bridgman-grown crystals are commonly selenium deficient. To overcome these problems, our group attempted to grow TMMs using a selenium vapor at a controlled pressure at low temperature [31, 32]. However, the driving force for growth was only supplied by the supersaturation induced by the concentration gradient and diffusion. Consequently, the growth speed was limited [33]. The crystal growth of transition metal phosphides using this technique have also been reported [34]; however, this research was limited to III-V compounds.

Here, we introduce an improved method based on gradual cooling, in which the TMM crystals are grown from a supersaturated solution formed by controlling the pressure of the chalcogen vapor. This method has the following advantages compared with the existing technique. Firstly, the pressure of the chalcogen vapor is controlled during growth thus maintaining the stoichiometry. Secondly, the growth rate is relatively high compared with that in the previous study [31]. Finally, the chemical composition of the solution depends only on temperature, so, by controlling the growth temperature, different specific compounds in the phase diagram can be precisely targeted [21]. In this study, we fabricated high-quality InSe and In₂Se₃ to demonstrate this method. We found the growth window for each compound and investigated the underlying mechanism.

2. Crystal Growth

We conducted crystal growth experiments using the different growth conditions listed in Table. 1. Let us take the successful growth of InSe and In₂Se₃ (conditions I and II) as examples to explain the growth procedure. A schematic diagram of the growth equipment is shown in Fig. 1. Ten grams of high purity selenium (5N, Kojundo Chemical Lab. Co., Ltd.) is placed at the bottom of the quartz ampoule. Then a 0.5 mm diameter quartz rod, which is smaller than the inside diameter of the quartz ampoule, is placed above the selenium ingots. The crucible, with 4 g of indium (6N, Dowa Co., Ltd.), is on top of the quartz rod. The ampoule is sealed after evaporation down to 10⁻⁶ Torr. Then the ampoule is placed in a vertical electrical furnace that has four separate temperature-controlled regions. Fig. 1a and 1b show the temperature profiles in the furnace during the growth of the crystals. The temperature at the crucible (T_G) and the bottom of the ampoule (T_V) are adjusted to control the growth temperature and the selenium vapor pressure. The equilibrium vapor pressure of pure selenium (P_V) is given by Baker's equation [35],

$$\log P_V (atm) = -\frac{5043}{T_V(K)} + 5.265 \quad (1)$$

The gap between the quartz rod and the ampoule is sufficiently narrow for the pressure of the selenium vapor at the crucible (P_G) to be described by the equation given by Nishizawa [36].

$$P_G = P_V \sqrt{\frac{T_G}{T_V}} \quad (2)$$

The crystal growth procedure is shown in Fig. 2a. There are four steps in the growth process. The growth temperature (T_G) with respect to the growth time is shown in Fig. 2b, and the temperature

(T_V) and pressure of the selenium vapor (P_G) with respect to the growth time are shown in Fig. 2c. Firstly, the temperature of the crucible is rapidly raised to a temperature higher than the growth temperature of InSe (Step I). Then the temperature is maintained for 10 hours to homogenize the solution (step II). Then we increase T_V to apply the specified pressure of the selenium vapor and this is maintained for 12 hours; the selenium vapor dissolves into the In solution until the solution becomes saturated at T_G if the pressure of the selenium vapor is higher than the equilibrium vapor pressure of the saturated solution at T_G (Step III). Finally, the crucible is gradually cooled at a rate of 1 °C/hour as shown in the inset of Fig. 2b, and the InSe crystal grows from the supercooled solution (Step IV). The pressure of the selenium vapor is maintained during step IV to prevent selenium evaporating from the solution. The whole system is cooled to room temperature after growth for 24 h. Likewise, the temperature and pressure profiles for the In_2Se_3 growth are shown in Fig. 2e and f.

3. Result and Discussion

Crystal growth was conducted at many different pressures and temperatures, and these are listed in Table. 1. The most promising conditions for the growth of InSe and In_2Se_3 are conditions I and II. In Fig. 3 we show the morphologies of an as-grown crystal of InSe. Fig. 3a shows the bottom of the ampoule, from where the pressure of the vapor is controlled, after growth. Some selenium remains, which means not all of this was used up during growth. A metallic looking bulk material with a length of about 3 cm was obtained from the crucible (Fig. 3b). The surface of this has stripes in one direction (Fig. 3c), indicating the direction of the (00n) plane [37]. Due to the random nucleation, each sample grows in an arbitrary direction compared to our previous samples grown

by the temperature difference method [31]. There are some bulges at the top of the ingot, which quickly react with hydrochloric acid, and these bulges were confirmed by inductively coupled plasma mass spectrometry (ICP-MS) to be pure selenium. This Se solidified when the crucible was cooled down to room temperature. After dissolving the metal in hydrochloric acid, a mirror-like surface was exposed (Fig. 3e). Microscope images of the surface are shown in Fig. 3e-h. The layer-stacking morphology can be observed in Fig. 3e. The six-fold symmetry of the surface structures are shown in Figs. 3f and g, and a terrace formed during growth is apparent in Fig.3h.

The crystal phases of the as-grown crystals were confirmed by x-ray diffraction (XRD) using a D8 ADVANCE (Bruker AXS Co., Ltd.). XRD spectra taken from different parts of the bulk crystal are shown in Fig. 4. For the XRD pattern of the sample grown using condition I, only the peaks with Miller indices of (00n) ($n = 3, 6, 9 \dots$) can be observed, which indicates the sample is InSe with R3m symmetry [38]. The lattice constants, $a = b = 4.1 \text{ \AA}$ and $c = 24.9 \text{ \AA}$, were derived from the strongest (006) peak at $2\theta = 21.3^\circ$. The XRD spectra of the sample taken 3, 6, and 9 mm from the bottom of the ingot are shown in Fig. 4b. Similarly, only the (00n) peaks can be seen in these spectra. The peak intensity decreases moving away from the bottom of ingot, for which we give the following explanation. The pressure of the selenium vapor is greater than the equilibrium pressure and this is continuously applied to the liquid surface during growth. The saturated selenium diffuses from the surface of the liquid towards the bottom of the crucible. The crystals are grown during cooling and the supersaturation increases as the temperature decreases. Consequently, there is excessive selenium in the solution. Unable to escape from the surface of the liquid, the selenium accumulates in the upper part of crucible. so that the crystal becomes indium deficient towards the top of the crystal, thereby affecting the peak intensity. The relationship between the full width at half maximum (FWHM) of the (0 0 15) peak and the distance

from the bottom of the sample where the peaks were observed is shown in Fig. 4c. The FWHM increases with the distance, which confirms that the crystallinity has been affected by the indium deficiency. The XRD pattern of the sample grown under condition II is shown in Fig. 4d, indicating the sample is In_2Se_3 with R3m (No. 166) symmetry [39]. Only (00n) peaks were observed in the XRD pattern, which indicates the sample is single crystal. The lattice constants, $a = b = 4.1 \text{ \AA}$ and $c = 28.8 \text{ \AA}$, were derived from the strongest (006) peak at $2\theta = 18.3^\circ$. XRD mapping from the bottom to 9 mm above the bottom of the bulk crystal is shown in Fig. 4e. These results suggest that the material is single crystal In_2Se_3 from the bottom up to 1 cm from the bottom. As shown in Fig. 4f, the FWHM of the (0 0 15) peak taken from the bottom of the bulk crystal is smaller than those taken from higher up. It is considered that the inhomogeneity of the selenium in the solution affects the growth of both InSe and In_2Se_3 .

The backscattered Raman spectra were taken using an NRS-5100 (JASCO Corp.) to confirm the polytypes of the as-grown samples. With excitation at 532 nm, the Raman spectra of samples grown under conditions I and II are shown in Fig. 5a and b, respectively. In the Raman spectrum of the sample grown under condition I, the transverse optical phonon $A_1(\text{TO})$ mode at 225 cm^{-1} verified that the sample is $\gamma\text{-InSe}$. The Raman modes E (176 cm^{-1}) and $A_1(\text{LO})$ (115 cm^{-1}) can also be seen in the spectrum. In the Raman spectrum of the sample grown under condition II, the E mode at 187 cm^{-1} and the strong $A_1(\text{TO})$ mode at 182 cm^{-1} indicate the material is $\alpha\text{-In}_2\text{Se}_3$ [40]. Moreover, the longitudinal optical phonon $A_1(\text{LO})$ mode at 244 cm^{-1} [41] and the $A_1(\text{LO}+\text{TO})$ mode at 104 cm^{-1} can also be seen in the spectrum. Raman spectra were also taken from different parts of the bulk crystal, showing modes only belonging to $\alpha\text{-In}_2\text{Se}_3$; so the crystal grown under condition II was confirmed as single crystal $\alpha\text{-In}_2\text{Se}_3$.

Because of the high vapor pressure of selenium, it is considered that Bridgman-grown indium selenide compounds are always non-stoichiometric. Here we measured the stoichiometry of the as-grown samples using inductive coupled plasma mass spectrometry (ICP-MS, Agilent 8800, Agilent Technologies, Ltd.). The results are shown in Table 1. With growth conditions I and II, the deviation from stoichiometric InSe and In₂Se₃ is less than 0.2 atomic percent. This is far smaller than a typical sample grown by the Bridgman technique [8, 37]. With the successful growth of InSe (conditions I, III, VI) and In₂Se₃ (conditions II, VII, VIII), it is expected that selenium vapor at a higher applied pressure will make the chemical ratio approach the stoichiometric ratio.

To explain these results, we propose a possible model in which the concentration of the supersaturated solution and the equilibrium vapor pressure are considered. The relationship between the concentration and the saturated vapor pressure can be described by Henry's law [42]:

$$P_{Se} = kc_{Se} \quad (3)$$

Here, P_{Se} and c_{Se} are the saturated vapor pressure and the concentration of Se, respectively. P_{Se} at a concentration of 60 at% is given by previously published results [43],

$$\log P_{Se} \text{ (Torr, } c_{Se} = 60 \text{ at\%)} = (8.056 \pm 0.96) - \frac{4949 \pm 170}{T_S(K)} \quad (4)$$

where T_S is the temperature of the saturated solution. The saturated selenium vapor pressure under different temperatures and concentrations can be obtained from Eqs. 3 and 4. P_{Se} as a function of c_{Se} and T_S is shown in Fig. 6a. If the pressure of the selenium vapor is higher than P_{Se} , the selenium will dissolve into the indium solution until the solution becomes saturated, or until the solution reaches the concentration where the pressure of the selenium vapor is equal to P_{Se} . Because the system has already reached equilibrium, the selenium will not continuously dissolve into the

solution even if it is not saturated. In the first situation, the crystal will be grown when slow cooling is started. Otherwise, crystals will not grow because the selenium concentration in the solution has not reached the saturated concentration. The temperature dependence of P_{Se} when c_{Se} is equal to 60 at% and 50 at%, indicating the stoichiometric ratios of InSe and In₂Se₃ are shown in Fig. 6b. The crystal growth conditions from I to IX are marked in the figure. $P_G > P_{Se}$ is satisfied with conditions I, II, and III, so samples with good crystallinity were obtained using these growth conditions. In contrast, with growth conditions IV, V, and IX, crystallization did not occur.

Note that the solution gradually cools down from the growth temperature over a period of 40 hours. The pressure of the selenium vapor may become larger than the vapor pressure at a specific temperature during cooling, so even when the pressure of the selenium vapor was smaller than P_{Se} , as with growth conditions VI and VIII, crystals were successfully grown. However, because there was insufficient time for the selenium to dissolve into the solution, the as-grown crystals were selenium deficient. On the other hand, P_{Se} is a linear approximation, so with growth condition III, it is considered the chemical ratio of the as-grown crystal differs slightly from stoichiometric InSe.

We have divided Fig. 6b into four areas, separated by the temperature of the liquid phase line between InSe and In₂Se₃ in the phase diagram [21]. The crystallization zone of InSe and In₂Se₃ is in the area of high P_{Se} . The growth windows of InSe and In₂Se₃ are indicated in the figure. Below the crystallization zone is the transitional zone, where the selenium can dissolve into the solution during the gradual cooling, and stoichiometric crystals can be grown. In the non-crystallization region, crystals cannot be grown due to the low pressure of the selenium vapor. Because the gradual cooling is conducted in a temperature zone within the liquid phase line in the In-Se phase diagram, only the single crystal of that component will grow in the crystallization zone. By

controlling the growth temperature (T_G) and the selenium vapor temperature (T_V) only, one can selectively grow indium selenide compounds without considering the selenium dose.

4. Conclusions

In this study, we introduced a novel crystal growth method for chalcogenide compounds, in which a saturated solution is produced by the application of the vapor of a chalcogen element, the pressure of which is controlled during the whole growth procedure, such that the growth temperature of this method is much lower than that of melt growth. Thus, the growth of non-stoichiometric crystals can be suppressed. Also, one can prepare the target crystal just by controlling the temperature without the need to consider the chemical composition of the solution in the crucible. We have successfully grown InSe and In₂Se₃ using this method. Moreover, we proposed a model to explain the growth mechanism and provide the growth windows of InSe and In₂Se₃. This method has the potential to be extended to the crystal growth of other transition metal chalcogenide compounds and benefit the preparation of samples for research into layered transitional metal chalcogenides.

Acknowledgments

This study is supported by Japanese society for promotion of science (JSPS) KAKENHI Grant number JP18J11396, JP19J20564, 20H02406.

FIGURES

Figure 1. (a) and (b): The temperature distributions for crystal growth conditions I and II (for the growth of InSe and In_2Se_3 respectively). (c): Schematic diagram of the quartz ampoule used in growth. The growth temperature (T_G) and the temperature of the selenium vapor are controlled according to the steps in the growth procedures.

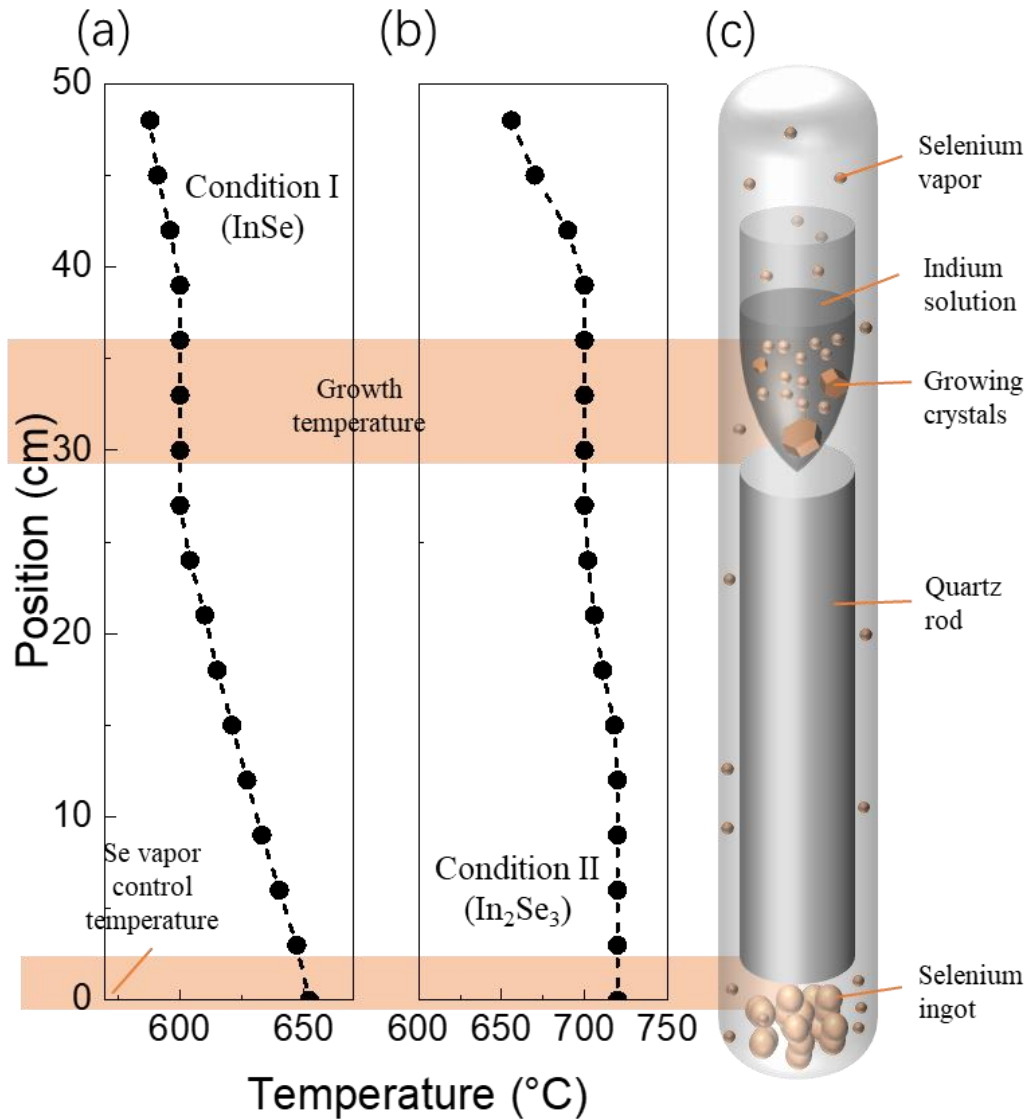
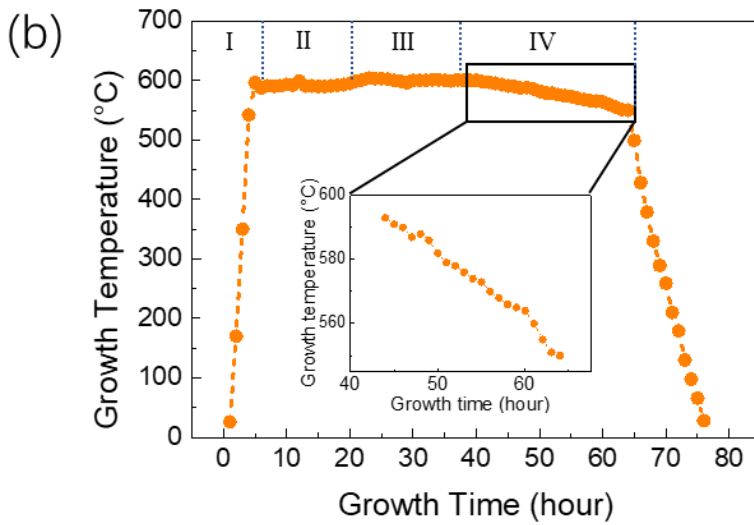
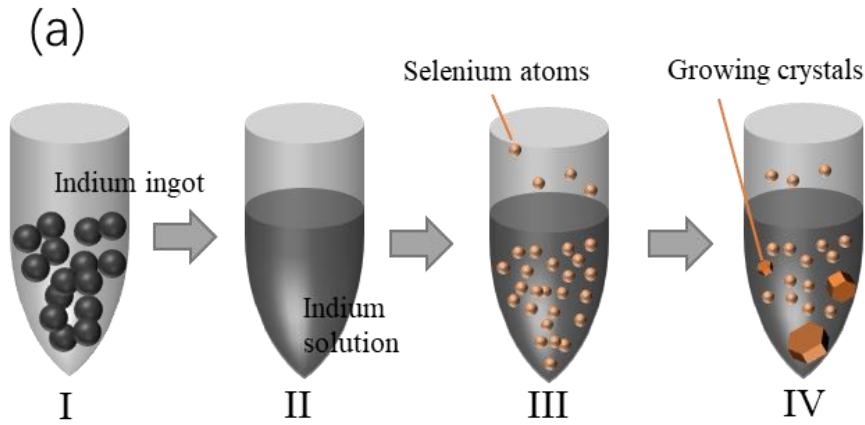
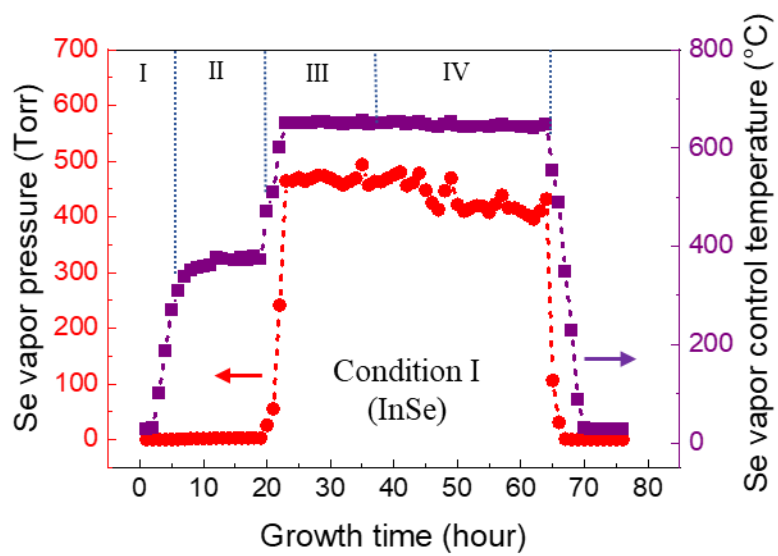


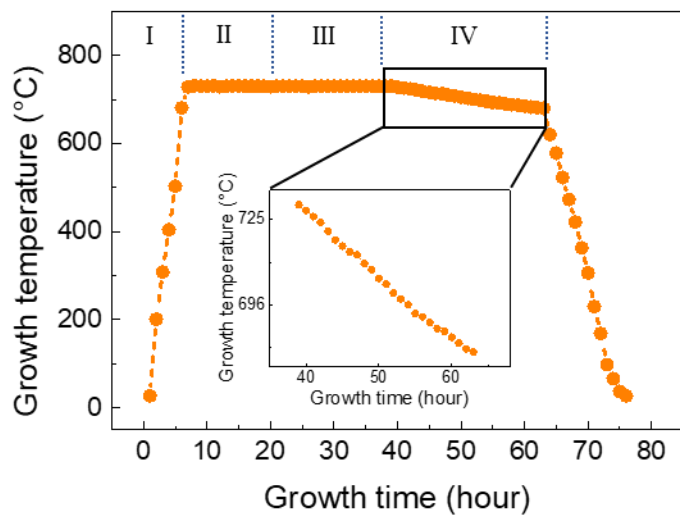
Figure 2. (a): Schematics of the four steps in the crystal growth procedure, I: setting the indium ingot in the crucible, II: melting and homogenizing the indium solution. III: application of the selenium vapor until the solution becomes saturated. IV: gradual cooling and crystal growth. (b): The growth temperature as a function of growth time for condition I. (Insert: The temperature during gradual cooling, the slope shows the cooling rate) (c) The time-dependent Se vapor control temperature and the pressure of the Se vapor in condition I. (d) and (e): the time-dependent T_G , T_V and P_G for growth condition II.



(c)



(d)



(e)

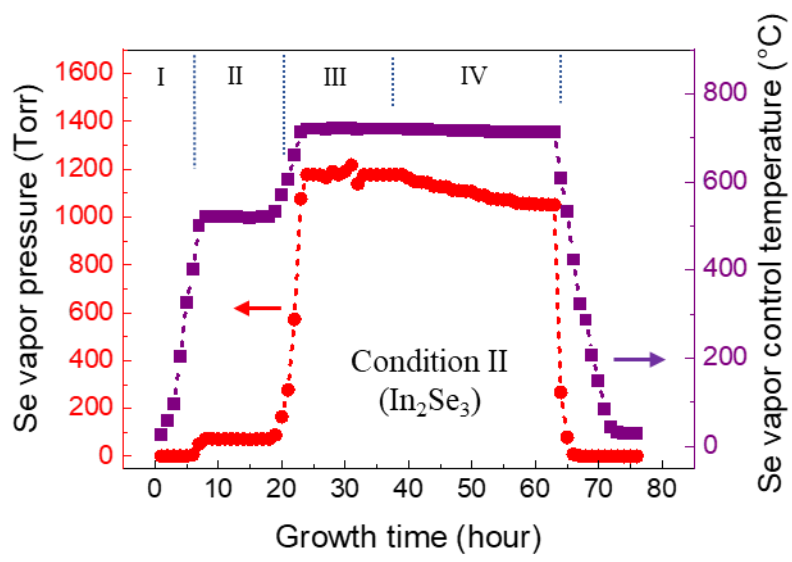


Figure 3. The morphology of the as-grown crystal grown using growth condition I, (a): The part of the ampoule from where the pressure of the selenium vapor is controlled. Some Se remains after growth. (b): The crucible after growth. (c): The ingot taken from the crucible. Condensed Se formed during cooling to room temperature remains at the top, below is the crystal. (d) Microscope image of the topside of the bulk crystal after removing the Se with hydrochloric acid. (e), (f) and (g): Microscope image of the surface perpendicular to the c-axis. Growth terraces can be seen in (g).

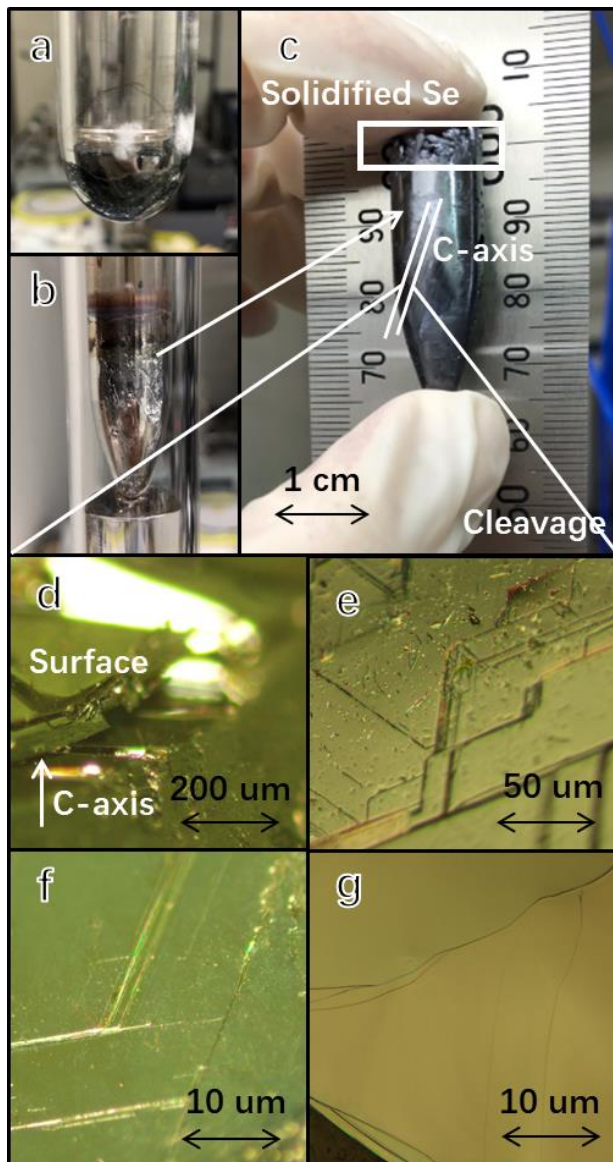
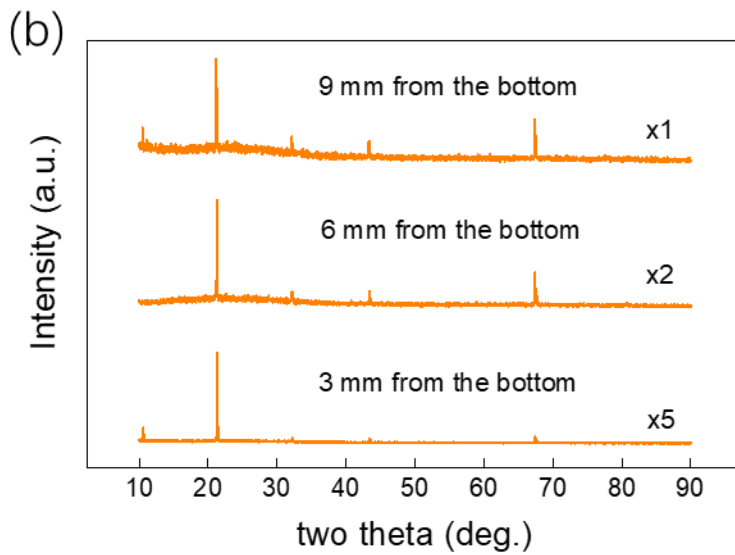
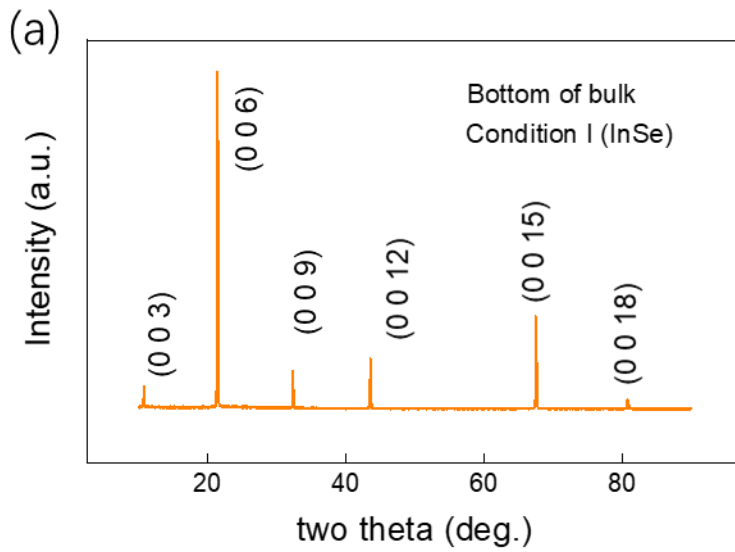
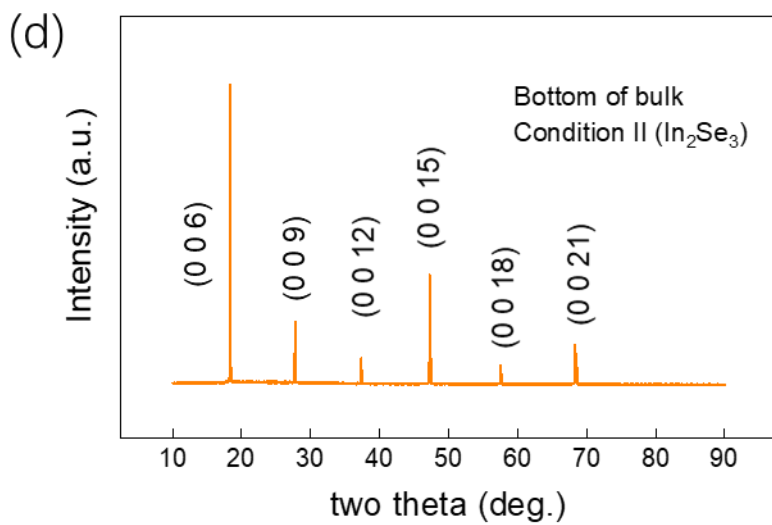
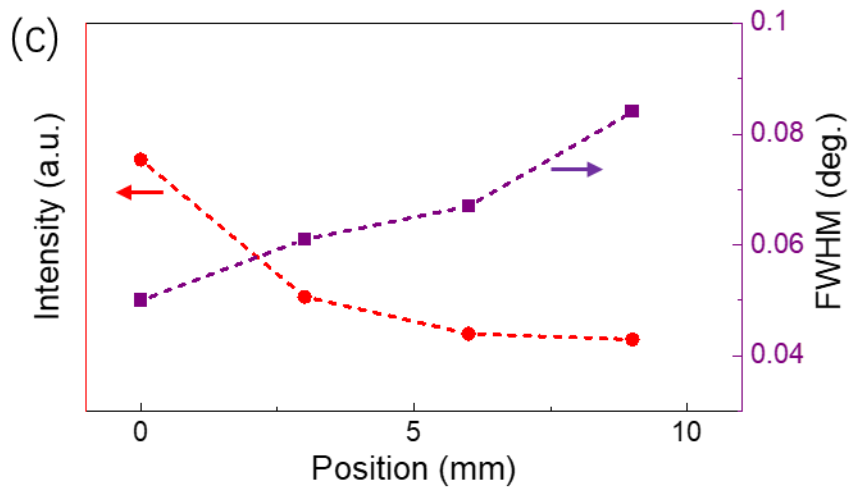


Figure 4. XRD patterns of as-grown crystals. (a): at the bottom of the bulk crystal grown using condition I (InSe). (b): at 3 mm, 6 mm, 9 mm from the bottom of the same sample. (c): the intensity and full width at half maximum (FWHM) of the (00 15) peak as a function of the distance from the bottom of the ingot. (d), (e) and (f): corresponding results for the crystal grown using condition II (In₂Se₃).





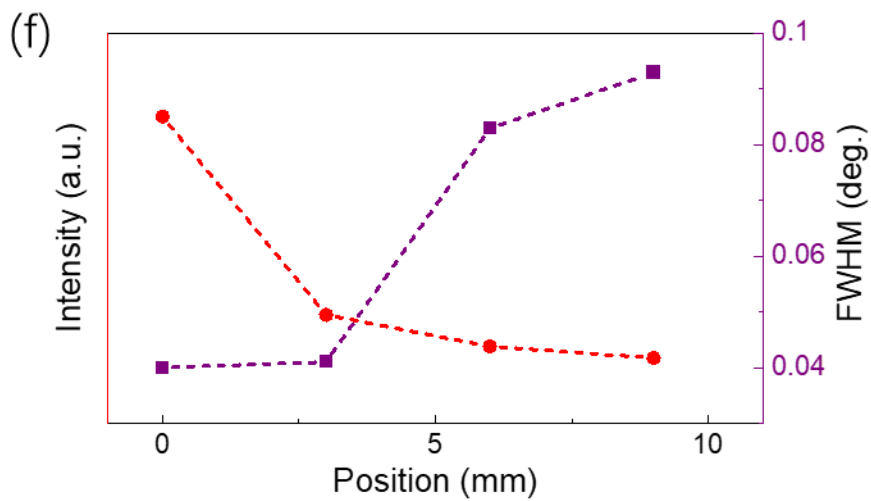
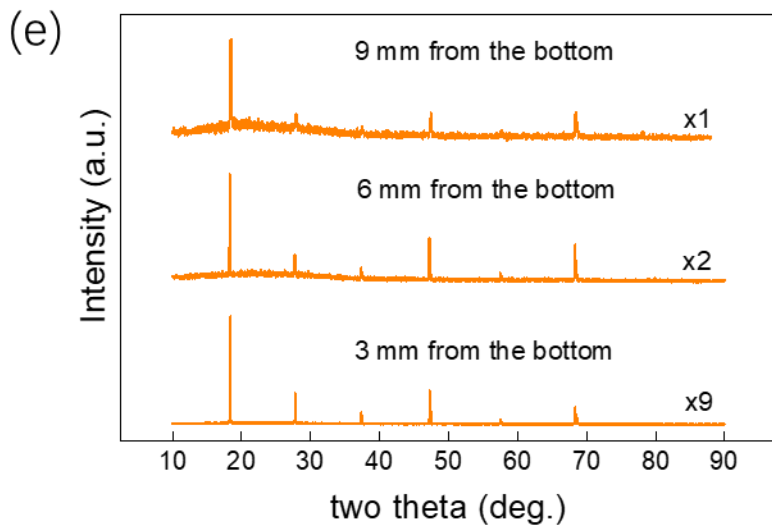
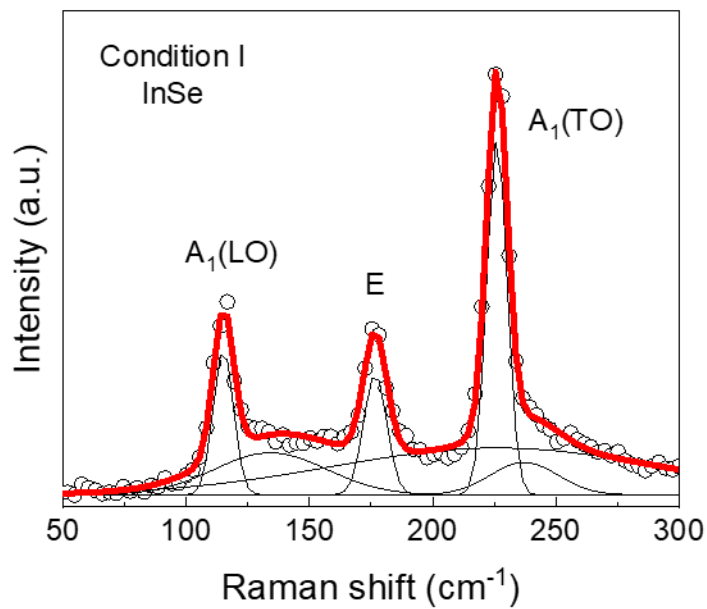


Figure 5. Backscattered Raman spectra of the sample grown using conditions I (a) and II (b)

(a)



(b)

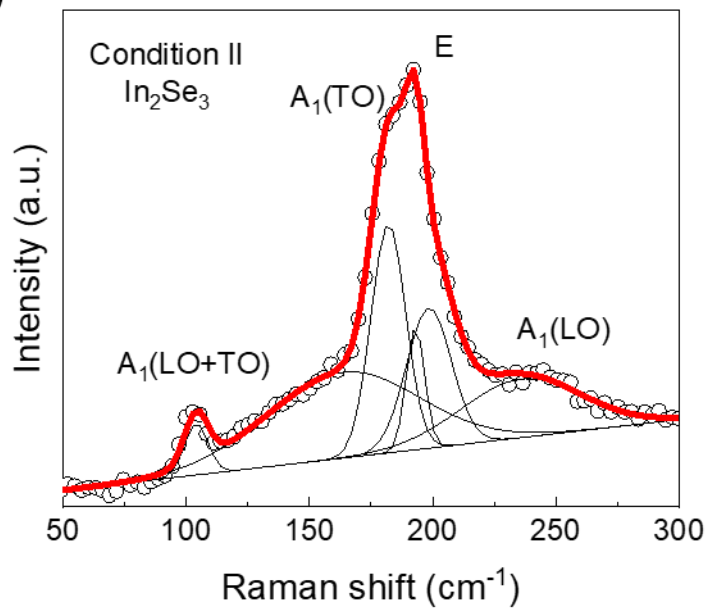
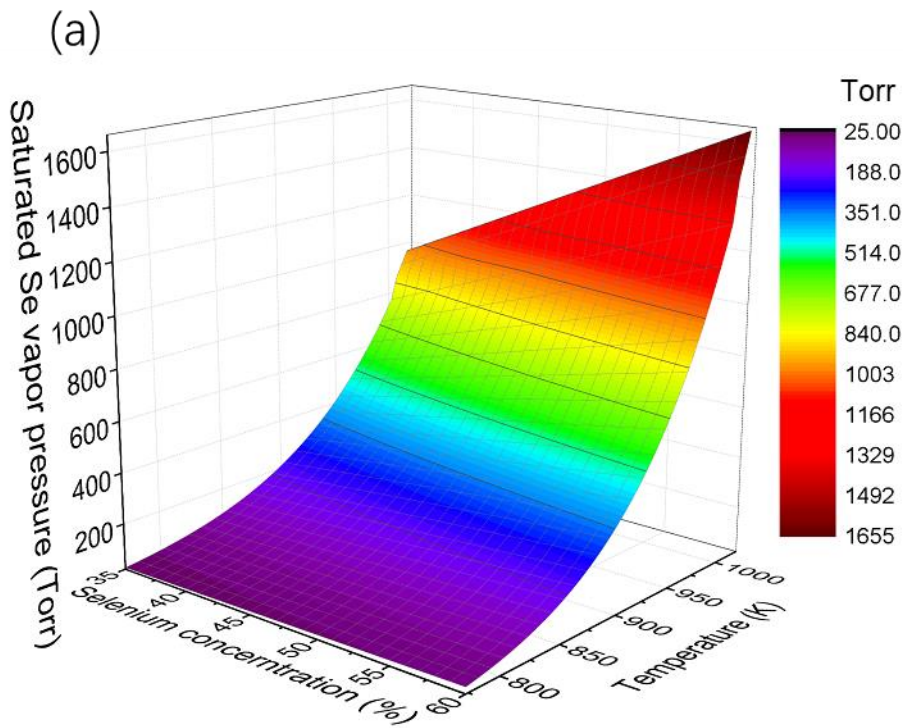
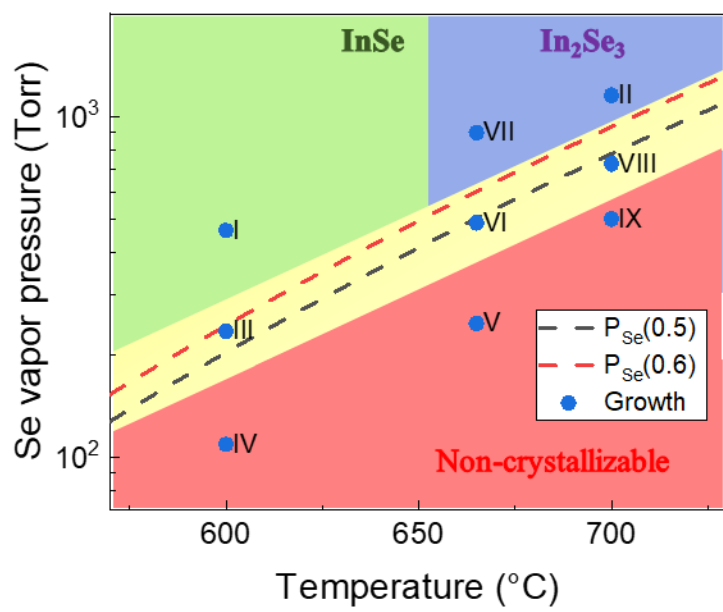


Figure 6. (a) the equilibrium selenium vapor pressure for different concentrations (P_{Se}) as a function of temperature. (b) The growth window for indium selenium compounds at different Se vapor pressures and temperature: the dashed line is the P_{Se} for 50 at% and 60 at% selenium concentrations. The growth experiments are marked by blue dots. The yellow part shows the transitional zone and the red region is the non-crystallizable zone.



(b)



TABLES.

Table 1. The growth conditions, as-grown crystal phases, and the stoichiometric properties of indium selenide compounds. The phases of the as-grown crystals were confirmed by Raman spectroscopy and XRD; the chemical composition of the indium and selenium were measured by ICP-MS.

No.	T_G (°C)	T_V (°C)	P_V (Torr)	P_G(Torr)	Crystal	In (at%)	Se (at%)
I	600	650	482	463	InSe	50.0	50.0
II	700	720	1170	1153	In₂Se₃	40.1	59.9
III	600	600	235	235	InSe	50.5	49.5
IV	600	550	105	109	In	100.0	0.0
V	665	600	235	247	In	82.3	17.7
VI	665	650	482	487	InSe	50.3	49.7
VII	665	700	920	896	In₂Se₃	40.6	59.4
VIII	700	680	716	726	In₂Se₃	42.1	57.9
IX	700	650	482	500	In	86.4	13.6

REFERENCES

- [1] J.-i. Nishizawa, T. Sasaki, Y. Oyama, T. Tanabe, Aspects of point defects in coherent terahertz-wave spectroscopy, *Physica B: Condensed Matter* 401-402 (2007) 677-681.
- [2] A. Kenmochi, T. Tanabe, Y. Oyama, K. Suto, J.-i. Nishizawa, Terahertz wave generation from GaSe crystals and effects of crystallinity, *Journal of Physics and Chemistry of Solids* 69(2-3) (2008) 605-607.
- [3] K. Saito, Y. Nagai, K. Yamamoto, K. Maeda, T. Tanabe, Y. Oyama, Terahertz Wave Generation via Nonlinear Parametric Process from ϵ -GaSe Single Crystals Grown by Liquid Phase Solution Method, *Optics and Photonics Journal* 04(08) (2014) 213-218.
- [4] Y. Sato, S. Zhao, K. Maeda, T. Tanabe, Y. Oyama, Electrical property and structural analysis of amphoteric impurity Ge doped GaSe crystal grown by liquid phase growth, *J. Cryst. Growth* 467 (2017) 34-37.
- [5] S.E. Al Garni, A.A.A. Darwish, Photovoltaic performance of TCVA-InSe hybrid solar cells based on nanostructure films, *Sol. Energy Mater. Sol. Cells* 160 (2017) 335-339.
- [6] N. Balakrishnan, Z.R. Kudrynskiy, E.F. Smith, M.W. Fay, O. Makarovskiy, Z.D. Kovalyuk, L. Eaves, P.H. Beton, A. Patanè, Engineering p-n junctions and bandgap tuning of InSe nanolayers by controlled oxidation, *2D Mater.* 4(2) (2017) 025043.
- [7] Z. Chen, J. Biscaras, A. Shukla, A high performance graphene/few-layer InSe photo-detector, *Nanoscale* 7(14) (2015) 5981-6.
- [8] W. Feng, J.-B. Wu, X. Li, W. Zheng, X. Zhou, K. Xiao, W. Cao, B. Yang, J.-C. Idrobo, L. Basile, W. Tian, P. Tan, P. Hu, Ultrahigh photo-responsivity and detectivity in multilayer InSe nanosheets phototransistors with broadband response, *Journal of Materials Chemistry C* 3(27) (2015) 7022-7028.
- [9] W. Feng, W. Zheng, W. Cao, P. Hu, Back gated multilayer InSe transistors with enhanced carrier mobilities via the suppression of carrier scattering from a dielectric interface, *Adv. Mater.* 26(38) (2014) 6587-93.
- [10] F. Moro, M.A. Bhuiyan, Z.R. Kudrynskiy, R. Puttock, O. Kazakova, O. Makarovskiy, M.W. Fay, C. Parmenter, Z.D. Kovalyuk, A.J. Fielding, M. Kern, J. van Slageren, A. Patane, Room Temperature Uniaxial Magnetic Anisotropy Induced By Fe-Islands in the InSe Semiconductor Van Der Waals Crystal, *Adv Sci (Weinh)* 5(7) (2018) 1800257.
- [11] K. Iordanidou, M. Houssa, J. Kioseoglou, V.V. Afanas'ev, A. Stesmans, C. Persson, Hole-Doped 2D InSe for Spintronic Applications, *ACS Applied Nano Materials* 1(12) (2018) 6656-6665.
- [12] C. Zhao, W. Gao, Q. Jiang, CO adsorption on metal doped 2D InSe: Mechanism and application, *Progress in Natural Science: Materials International* 29(3) (2019) 305-309.
- [13] X. Yin, J.Y. Liu, L. Chen, L.M. Wu, High Thermoelectric Performance of In₄Se₃-Based Materials and the Influencing Factors, *Acc. Chem. Res.* 51(2) (2018) 240-247.
- [14] B. Abay, H. Efeoğlu, Y. Yoğurtçu, Low-temperature photoluminescence of n-InSe layer semiconductor crystals, *Mater. Res. Bull.* 33(9) (1998) 1401-1410.
- [15] S. Ashokan, K.P. Jain, M. Balkanski, C. Julien, Resonant Raman scattering in quasi-two-dimensional InSe near the M₀ and M₁ critical points, *Phys. Rev. B* 44(20) (1991) 11133-11142.
- [16] O.A. Balitskii, V.P. Savchyn, V.O. Yukhymchuk, Raman investigation of InSe and GaSe single-crystals oxidation, *Semicond. Sci. Technol.* 17 (2002) L1.
- [17] D.A. Bandurin, A.V. Tyurnina, G.L. Yu, A. Mishchenko, V. Zolyomi, S.V. Morozov, R.K. Kumar, R.V. Gorbachev, Z.R. Kudrynskiy, S. Pezzini, Z.D. Kovalyuk, U. Zeitler, K.S.

- Novoselov, A. Patane, L. Eaves, I.V. Grigorieva, V.I. Fal'ko, A.K. Geim, Y. Cao, High electron mobility, quantum Hall effect and anomalous optical response in atomically thin InSe, *Nat Nanotechnol* 12(3) (2017) 223-227.
- [18] C.D. Blasi, D. Manno, S. Mongelli, A. Rixzzo, Electron Diffraction Study of Melt-Grown InSe Crystals, *Il Nuovo Cimento* 7 (1986) 795-806.
- [19] B. Gürbulak, M. Kundakçi, A. Ateş, M. Yildirim, Electric field influence on exciton absorption of Er doped and undoped InSe single crystals, *Phys. Scr.* 75(4) (2007) 424-430.
- [20] B. Gürbulak, M. Şata, S. Dogan, S. Duman, A. Ashkhasi, E.F. Keskenler, Structural characterizations and optical properties of InSe and InSe:Ag semiconductors grown by Bridgman/Stockbarger technique, *Physica E: Low-dimensional Systems and Nanostructures* 64 (2014) 106-111.
- [21] K. Imai, K. Suzuki, T. Haga, Y. Hasegawa, Y. Abe, Phase diagram of In-Se system and crystal growth of indium monoselenide, *J. Cryst. Growth* 54(3) (1981) 501-506.
- [22] S. Jandi, C. Carlon, Raman Spectrum of Crystalline InSe, *Solid State Commun.* 25 (1978) 5-8.
- [23] S. Shigetomi, T. Ikari, Optical and Electrical Properties of Layer Semiconductor n-InSe Doped with Sn, *Jpn. J. Appl. Phys.* 41(Part 1, No. 9) (2002) 5565-5566.
- [24] S. Shigetomi, T. Ikari, H. Nakashima, Impurity level in p-type layered semiconductor InSe doped with Hg, *phys. stat. sol. (b)* 209 (1998) 93.
- [25] S.R. Tamalampudi, Y.Y. Lu, U.R. Kumar, R. Sankar, C.D. Liao, B.K. Moorthy, C.H. Cheng, F.C. Chou, Y.T. Chen, High performance and bendable few-layered InSe photodetectors with broad spectral response, *Nano Lett.* 14(5) (2014) 2800-6.
- [26] M. Zolfaghari, K.P. Jain, H.S. Mavi, M. Balkanski, C. Julien, A. Chevy, Raman investigation of InSe doped with GaS, *Mater. Sci. Eng., B* 38 (1996) 161-170.
- [27] A. Chevy, Improvement of growth parameters for Bridgman-grown InSe crystal, *J. Cryst. Growth* 67 (1984) 119-124.
- [28] P.H. Ho, Y.R. Chang, Y.C. Chu, M.K. Li, C.A. Tsai, W.H. Wang, C.H. Ho, C.W. Chen, P.W. Chiu, High-Mobility InSe Transistors: The Role of Surface Oxides, *ACS Nano* 11(7) (2017) 7362-7370.
- [29] A. Politano, G. Chiarello, R. Samnakay, G. Liu, B. Gurbulak, S. Duman, A.A. Balandin, D.W. Boukhvalov, The influence of chemical reactivity of surface defects on ambient-stable InSe-based nanodevices, *Nanoscale* 8(16) (2016) 8474-9.
- [30] H. Xu, W. Wang, Y. Zhao, X. Zhang, Y. Feng, J. Tu, C. Gu, Y. Sun, C. Liu, Y. Nie, I.C. Edmond Turcu, Y. Xu, L. He, Temperature-induced band shift in bulk γ -InSe by angle-resolved photoemission spectroscopy, *AIP Advances* 8(5) (2018) 055123.
- [31] C. Tang, Y. Sato, T. Tanabe, Y. Oyama, Low temperature liquid phase growth of crystalline InSe grown by the temperature difference method under controlled vapor pressure, *Journal of Crystal Growth* 495 (2018) 54-58.
- [32] T. Tanabe, C. Tang, Y. Sato, Y. Oyama, Direct determination of the interlayer van der Waals bonding force in 2D indium selenide semiconductor crystal, *Journal of Applied Physics* 123(24) (2018) 245107.
- [33] T. Tanabe, S. Zhao, Y. Sato, Y. Oyama, Effect of adding Te to layered GaSe crystals to increase the van der Waals bonding force, *J. Appl. Phys.* 122(16) (2017) 165105.
- [34] A. Yamamoto, C. Uemura, InP Single Crystal Growth by the Synthesis, Solute Diffusion Method, *Jpn. J. Appl. Phys.* 17(10) (1978) 1869-1870.

- [35] E.H. Baker, The vapour pressure and resistivity of selenium at high temperatures, *Journal of the Chemical Society A* 0 (1968) 1089.
- [36] N. Jun-ichi, K. Yutaka, O. Yasuo, Balance method for experiments under controlled vapor pressure, *Jpn. J. Appl. Phys.* 19 (1980) 345.
- [37] M. Wu, Q. Xie, Y. Wu, J. Zheng, W. Wang, L. He, X. Wu, B. Lv, Crystal structure and optical performance in bulk γ -InSe single crystals, *AIP Advances*, American Institute of Physics Inc., 2019, p. 025013.
- [38] S. Popović, A. Tonejc, B. Gržeta-Plenković, B. Čelustka, R. Trojko, Revised and new crystal data for indium selenides, *J. Appl. Crystallogr.*, International Union of Crystallography (IUCr), 1979, pp. 416-420.
- [39] B. Gržeta, S. Popović, N. Cowlam, B. Čelustka, Low-temperature X-ray diffraction examination of In₂Se₃, *J. Appl. Crystallogr.* 23(4) (1990) 340-341.
- [40] R. Lewandowska, R. Bacewicz, J. Filipowicz, W. Paszkowicz, Raman scattering in α -In₂Se₃ crystals, *Mater. Res. Bull.* 36(15) (2001) 2577-2583.
- [41] K. Kambas, J. Spyridelis, Far Infrared optical study of α -In₂Se₃ compound, *Mater. Res. Bull.* 13(7) (1978) 653-660.
- [42] III. Experiments on the quantity of gases absorbed by water, at different temperatures, and under different pressures, *Philos. Trans. R. Soc. London*, The Royal Society, 1803, pp. 29-274.
- [43] A.M. Klimova, V.A. Ananichev, A.I. Demidov, L.N. Blinov, Investigation of the saturated vapor pressure of selenium and indium sesquiselenide In_{0.4}Se_{0.6}, *Glass Phys. Chem* 32(4) (2006) 436-438.